journal of the mechanical behavior of biomedical materials 144 (2023) 105937

Contents lists available at ScienceDirect

Journal of the Mechanical Behavior of Biomedical Materials

journal homepage: www.elsevier.com/locate/jmbbm

Fabrication and characterisation of bioglass and hydroxyapatite-filled scaffolds

Laura Mendoza-Cerezo [a], Jesús M. Rodríguez-Rego [a,*], Anabel Soriano-Carrera [a], Alfonso C. Marcos-Romero [a], Antonio Macías-García [b]

[a] Departamento de Expresión Gráfica, Escuela Técnica Superior de Ingenieros Industriales, Universidad de Extremadura, Avenida de Elvas, s/n, 06006, Badajoz, España
[b] Departamento de Ingeniería Mecánica, Energética y de Materiales, Escuela Técnica Superior de Ingenieros Industriales, Universidad de Extremadura, Avenida de Elvas, s/n, 06006, Badajoz, España

ARTICLE INFO

Keywords:
Biofabrication
Bioglass
PLA
Hydroxyapatite
Scaffold

ABSTRACT

Tissue engineering is a continuously evolving field. One of the main lines of research in this field focuses on the replacement of bone defects with materials designed to interact with the cells of a living organism in order to provide the body with a structure on which new tissues can easily grow. Among the most commonly used materials are bioglasses, which are frequently used due to their versatility and good properties. This article discusses the results of the production of an injectable paste of Bioglass® 45S5 and hydroxyapatite on a 3D printed porous structure by additive manufacturing, using a thermoplastic (PLA). The results were evaluated in a specific application of the paste, so the mechanical and bioactive properties were studied to show the multiple possibilities of using this combination for its application in regenerative medicine and more specifically in bone implants.

1. Introduction

Tissue engineering is a branch of bioengineering that offers very interesting solutions for tissue and organ procurement in regenerative medicine by combining cells, growth factors, biomaterials and 3D printing technology to fabricate biological constructs (Langer and Vacanti, 1993). When tissues are injured or diseased, regeneration is in many cases not possible, and the use of permanent implants is limited. This causes a serious problem, mainly because of the need for organ transplantation for many patients (Langer and Vacanti, 1993) or because of the long waiting times for recovery of some tissues, such as bone tissue.

Our body has two mechanisms for wound healing: by repair or by regeneration (Langer and Vacanti, 1993). The problem arises when our organism, and more specifically the bone, is unable to regenerate the damaged structure. It is at this point that tissue engineering must develop methods that overcome the organism's capacity to spontaneously regenerate tissues (Langer and Vacanti, 1993; "Objetivos conceptuales y metodológicos de, 1575; Schneider et al., 2010; Cuende, 2013).

Tissue engineering is postulated as a fundamental tool, with the capacity to solve, in the future, the problems derived from the regeneration of any type of tissue together with 3D printing, allowing these tissues to adapt to the necessary morphology (Mavili et al., 2007; Faber et al., 2006; D'urso et al., 2000; Shor et al., 2009).

Currently, most implants are made of materials that are much more resistant than bone, such as metals. These implants cannot adapt to changing physiological conditions. Therefore, better substitutes such as synthetic biomaterials are needed (Fu et al., 2011a). A biomaterial is a material intended to interact with biological systems to assess, treat, augment or replace a tissue or organ. In addition, they can be 3D printed to be used as structural materials for scaffolds ("The Williams Dictionary of Biomaterials, 2021).

A scaffold is a material designed to interact with the cells of a living organism to provide the body with a structure on which new tissue can easily grow (Fávaro-Pípi et al., 2011). Scaffolds, as an indispensable part of tissue engineering, are versatile in promoting cell-scaffold interactions, cell adhesion and extracellular matrix secretion. They also enable the transport of nutrients, debris and regulatory signals to allow cell proliferation and differentiation (Wang et al., 2023). To achieve this characteristic, high porosity is required, with sufficiently large pore size. This facilitates cell adhesion and diffusion in the structure, useful also

* Corresponding author.
E-mail address: jesusrodriguezrego@unex.es (J.M. Rodríguez-Rego).

https://doi.org/10.1016/j.jmbbm.2023.105937
Received 9 March 2023; Received in revised form 23 May 2023; Accepted 24 May 2023
Available online 6 June 2023

for nutrient supply. Sometimes also biodegradability is an important factor, to allow the natural tissue to regain all its former structure. Scaffolds are commonly used to repair bone damage, and are a valid alternative to grafting (Baino and Vitale-Brovarone, 2011).

Scaffolds made of bioinert and biodegradable materials filled with bioglass are a very good option as they have mechanical properties similar to those of natural bone. They have good bioactivity, i.e., they have a high capacity to interact chemically with tissues. In addition, bioglass forms a silica gel very quickly in a biological environment, and on that layer calcium phosphates, the mineral part of bone, can strongly adhere and grow. One of the most widely used, due to its optimal bioactivity, is a bioactive glass called Bioglass® 45S5 (Baino and Vitale-Brovarone, 2011), (Li et al., 1991).

On the other hand, scaffolds filled with natural inorganic components have circumstantial biological or physiological functions. An example is hydroxyapatite (HA), which is the main component of bones and teeth (Wang et al., 2023). Bioceramics such as hydroxyapatite are composed of calcium phosphate, which has positive effects on osteoblast proliferation and adhesion, due to its chemical structure comparable to that of human bone (Filová et al., 2014).

Our aim is to design a 3D printed biodegradable hollow cube of PLA and its subsequent filling by injection of a paste based on bioglass and hydroxyapatite with good mechanical properties and high bioactivity (Baino and Vitale-Brovarone, 2011), in order to consider its use in tissue engineering for bone implants (Li et al., 1991).

2. Materials and methods

2.1. Starting materials

The following starting materials have been used for this work:

2.1.1. Bioglass® 45S5 commercial bioactive glass

Commercial bioactive glasses are ceramic materials with a chemical composition that induces and conducts tissue mineralisation. They are therefore of great interest due to their excellent bioactivity and biocompatibility, as well as being available in different families with different compositions (Aguilar-Reyes et al., 2012).

Bioactive glass 45S5 was developed by Hench in 1971 by fusing a mixture of oxides in the following proportions: 45% SiO_2, 24.5% Na_2O, 24.5% CaO and 6% P_2O_5 (weight percentage) (Hench et al., 1971). Its name is due to the SiO2 content (45% by weight) and the Ca/P molar ratio (5% by weight). This material is most commonly used in clinical applications (dentistry, bone regeneration, ear prostheses, etc.) (Poh et al., 2013), (Farooq et al., 1001).

Bioactive glass can be obtained by the sol-gel process. This technique allows to control the composition and homogeneity of the glass, due to the low working temperature required (Li et al., 1991), (Hench, 2013), (Jonasova et al., 2002).

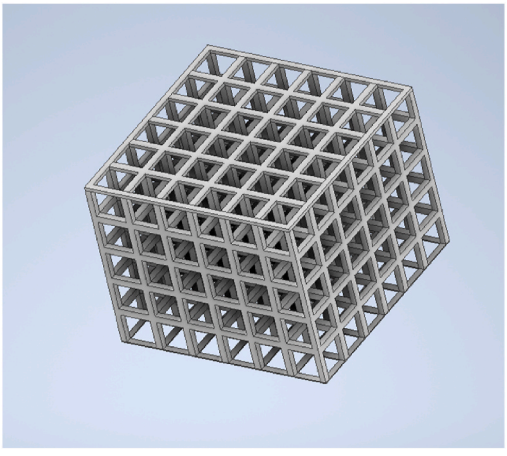

Fig. 1. Cube design for 3D printing where you can see the spaces that will be filled with the pastes studied in this work.

2.1.2. Polyvinyl alcohol (PVA)

Polyvinyl alcohol (PVA), also called polyethenol or poly (vinyl alcohol), is a water-soluble synthetic polymer with the general chemical formula (C_2H_4O). It has excellent film-forming, emulsifying and adhesive properties. It is also resistant to oil, grease and solvents. It is odourless and non-toxic with high barrier properties for oxygen and flavours. However, these properties are moisture-dependent, i.e., the higher the moisture, the more water is absorbed. Water, which acts as a plasticiser, will in turn reduce its tensile strength, but increase its elongation and tear strength. PVA is fully degradable and dissolves quickly.

2.1.3. Hydroxyapatite (HA)

Hydroxyapatite ($Ca_{10}(PO_4)_6(OH)_2$) is a compound of great interest in the field of biomedicine, because it has characteristics that make it suitable for use in bone regeneration. These characteristics are its bioactivity, exceptional biocompatibility, biodegradability, osteoconductivity and lack of toxicity, in addition to being an inorganic, non-inflammatory and non-immunogenic material (Salahuddin et al., 2022). Furthermore, under physiological conditions, hydroxyapatite (HA) is the most stable crystalline form of calcium phosphate. These characteristics are due to its chemical composition, which mimics the inorganic components of human teeth and bone (Qi et al., 2014). This makes HA biocompatible and it can be firmly combined with natural bone (Bai et al., 2018).

2.1.4. Polylactic acid (PLA)

PLA is a thermoplastic, biodegradable and biocompatible biopolymer that is widely used in medical applications. This material has a high tensile strength and low elongation, which gives it a high Young's modulus. This makes it a very suitable material for load-bearing applications such as sutures and orthopaedic fixations ("Injertos sustitutos no óseos, 1699).

High-resolution PLA structures for medical purposes can be obtained by 3D printing with a nozzle-based system.

2.2. Characterisation of commercial Bioglass ® 45S5

The 45S5 bioglass was characterised by X-ray diffraction and FT-IR spectrophotometry.

2.2.1. X-ray diffractogram

X-ray diffraction is a powerful non-destructive technique for characterizing crystalline materials (Sima et al., 2016) based on the constructive interference of monochromatic X-rays generated by a cathode ray tube, filtered to produce monochromatic radiation, collimated to concentrate them and directed towards the crystalline sample. This interaction of the incident rays with the crystal causes them to diffract in a pattern determined by the position, arrangement and size of the crystal components (Donnelly et al., 2011).

The samples were analysed by X-ray crystallography, using a Rigaku "MiniFlex+" tabletop X-ray diffractometer and an XPERT-PRO system, in which the X-rays were formed by a copper ampoule subjected to a potential of 45 kV and a current of 40 mA. The scanning (2θ) was performed between 20° and 60-90°, with steps of 0.0334225°. Thus, X-ray diffraction is a useful technique for the analysis of the crystallinity of solid samples.

2.2.2. FT-IR spectrophotometry

Fourier transform infrared (FT-IR) is one of the most important analytical techniques for researchers because this type of analysis can be used to characterise samples in the form of liquids, solutions, pastes,

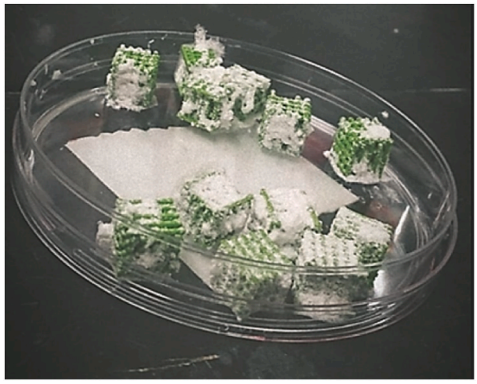

Fig. 2. Tests for filling the 3D cubes with the different pastes.

powders, films, fibres and gases (Nandiyanto et al., 2019).

In the FTIR analysis procedure, samples are exposed to infrared (IR) radiation. The IR radiation then impacts the atomic vibrations of the sample molecule, causing specific absorption and/or energy transfer, which makes FTIR useful for determining the specific molecular vibrations contained in the sample (Wang and Wang, 2009).

For the analysis of the samples by infrared spectroscopy, a Thermo Scientific Nicolet 6700 FT-IR spectrophotometer was used. For this, tablets were prepared by adding 1 mg of sample to 200 mg of KBr, and pressing the powders with the help of a 13 mm diameter SPECAC mould. Subsequently, the infrared spectrum obtained was analysed, identifying the characteristic absorption bands and comparing them with available references and databases.

2.3. Sample preparation

A hollow 3D cube model was designed with PLA by 3D printing (Fig. 1) to be filled by injection moulding with a paste as shown in Fig. 2.

The filler paste was obtained by mixing a bioactive glass (BGP) consisting of 45S5 bioactive glass with 95% PVA and H_2O (20% PVA, 80% H_2O) and HA hydroxyapatite in the following proportions:

- 25% BGP/75% HA (sample 1)
- 50% BGP/50% HA (sample 2)
- 75% BGP/25% HA (sample 3)

2.4. Characterisation of the samples (BGP + HA)

The prepared samples were characterised by determining viscosity, setting time and bioactivity.

2.4.1. Viscosity and setting time

The viscosity of a fluid is a measure of its resistance to flow. It describes the internal friction of a moving fluid. Viscous fluids resist movement because their molecular composition creates a lot of internal friction, while fluids with low viscosity flow easily because their molecular composition creates little friction when in motion.

A viscometer was used to determine the viscosity, and the setting time was determined using the line-drawing and gap-filling method with the manufactured pastes.

The viscosity was measured using the HAAKE RV2 MK 500 viscometer. For this purpose, the sample was introduced into the viscometer and the system was subjected to different angular velocities. The measured values were calculated manually, and the viscosity curve was obtained in Excel.

The characteristic equation for non-Newtonian fluids is the power law (equation (2.1)):

$$\mu_{eff=K}\left[\frac{\partial\mu}{\partial y}\right]^{n-1} \tag{2.1}$$

Where:

μ_{eff} is the apparent or effective viscosity.
$\frac{\partial\mu}{\partial y}$ is the shear velocity.
n is the empirical flow behaviour index.
K is the consistency index.

From the representation of the apparent or effective viscosity as a function of shear rate, the values of K and n can be determined. The value of K and n can be obtained from the equation $log(\mu_{eff})$ and $log\ \frac{\partial\mu}{\partial y}$. The slope line gives the value of n-1 from which n can be calculated. The intersection at $log\ \frac{\partial\mu}{\partial y} = 0$ gives the value of K.

The cohesion and setting times of the specimens were determined by the following tests:

- Cohesion time (CT): time elapsed from when the sample is deposited until it acquires a consistency such that, without having hardened completely, it can be injected. To determine the cohesion time, a line is drawn on a piece of paper with a syringe filled with sample and the time elapsed until the line drawn on the paper acquires a certain consistency and no longer sticks to the glove when touched is measured.
- Setting time (ST): The time elapsed from the start of mixing and loading into a syringe until the mass has acquired the necessary firmness, consistency, hardness and strength to prevent the sample from flowing through it. To determine the setting time, holes are created in a surface, and the syringe filled with sample until the sample no longer fills the holes created. This time will indicate that the sample is no longer flowing.

2.5. PLA scaffold 3D printing

Polymers are widely used biomaterials for 3D printing. Specifically, PLA polymers are mainly used in FDM printers, as fused deposition modelling is a cost-effective method to create scaffolds with controlled porosity and architecture. Scaffold design directly affects mechanical properties, cell response, permeability and nutrient diffusion (Serra et al., 2013). For this purpose, a cube-shaped scaffold was designed with Autodesk Fusion. The model was translated into g-code using Cura software. Based on this, a cube-shaped scaffold (1 cm × 1 cm x 1 cm) was manufactured by 3D printing (standard 3D printer, Ender 3) with *Smartfil* PLA filament from *Smart Materials* 3D. This PLA filament offers excellent mechanical properties and high quality in 3D printing. Each cube has six layers, and each layer is made with 6 parallel lines (Fig. 1).

2.5.1. Characterisation of the scaffold

2.5.1.1. Porosity. To determine the porosity of the cube-shaped scaffold, its $\rho_{scaffold}$ density was calculated using the mass and volume of the 3D printed cubes. The porosity p was calculated with the formula:

$$p = 1 - \frac{\rho_{scaffold}}{\rho_{PLA}} \tag{2.4}$$

where = 1.25 g/cm^3 is the theoretical density of PLA.

2.5.1.2. Mechanical properties of the scaffold (hollow PLA cube). The compressive strength test consists of applying a constant load on a specimen along its vertical axis, in which the load bridge descends at a constant speed, compressing the piece between the compression plates.

The *Simadzu* Autograph universal mechanical testing machine with a

maximum load capacity of 50 kN, computer-controlled by means of the *Shimadzu Trapezium* application, is used to carry out the tests. This machine allows tensile, bending and compression tests to be performed, using the corresponding heads for each test.

Before performing the tests, the test parameters are configured manually using the computer connected to the machine. Values such as specimen dimensions, test speed (in this case 1 mm/min) and maximum displacement (in this case 1 mm) are entered).

To test the compressive strength of the PLA-printed cubes, pressure was applied to the cubes with the universal mechanical testing machine up to the previously configured point, and both the result recorded by the machine and the state of the cube were observed.

2.6. Hollow cube scaffold filling and characterisation

From the pastes (BGP + HA) prepared with different proportions of HA, 3D PLA cubes were filled, as shown in Fig. 2.

2.6.1. Mechanical properties of the filled scaffold

To perform compression tests with the pastes injected into the PLA scaffold, a Shiadzu AG-IS machine was used and the stress vs. strain curves were determined.

2.6.2. Bioactivity test of samples

The concept of bioactivity arises from the ability of some bioactive glasses to spontaneously form bonds with bone. One of the methods to evaluate the bioactivity of materials is to immerse the material in a liquid medium with characteristics similar to those of physiological fluids. Kokubo (1991) determined that in order to create a direct bond between the bone and the material, the formation of an apatite layer on the material once implanted in the human body is necessary. In order to reproduce this formation in humans, a Simulated Body Fluid (SBF) was used. The bioactivity of a material can be predicted by the formation of apatite on the surface, so that the formation of apatite in these materials, when immersed in SBF, correlates well with their bioactive behaviour in vivo studies (Kokubo and Takadama, 2006). For the bioactivity test, SBF with an ion concentration approximately equal to that of human blood plasma has been used (Li et al., 1991), (Hench, 2013), (Jonasova et al., 2002).

The bioactivity test was carried out by contacting the prepared samples with 20 ml of SBF for different periods of time (1, 3, 5 and 7 days).

Bioactivity evaluation was performed using scanning electron microscopy (SEM) to obtain images of the Surface.

2.6.2.1. Scanning electron microscopy (SEM). By imaging the samples by scanning electron microscopy, it is possible to observe the morphological evolution of the surface, the macroporosity and microporosity, as well as the presence of apatite. To determine the bioactivity of the samples, an SEM equipment model Quanta 3D FEG//FEI Company has been used.

3. Results

3.1. Characterisation of commercial Bioglass ® 45S5

The bioactivity of 45S5 is based on its low SiO_2 content and high Na_2O and CaO content, as well as the CaO/P_2O_5 ratio (Jones, 2015).

X-ray diffraction was applied to the 45S5 bioglass particles to obtain a structural analysis of the particles. FT-IR spectroscopy allows us to understand the structure of the 45S5 bioglass powders by determining the vibrations of the different groups on the surface of the sample.

The X-ray diffractogram (XRD) of the 45S5 bioglass powders shows in Graph 1 that the material has a crystalline structure due to the number of peaks corresponding to the formation of crystals.

The peaks corresponding to $Na_2CaSi_2O_6$ are related to the treatment of the sintering material and start to form at around 6000 °C (Rámila and Vallet-Regí, 2001). These characteristic peaks are located at 2θ of 22.4°, 23.4°, 24.8°, 32.6°, 33.1°, 33.8°, 34.4° and 42.3°.

Other peaks corresponding to the crystalline phase combeite (mineral with formula $Na_2Ca_2Si_3O_9$) are also observed, probably related to the high sintering temperatures of the bioglass (Sanders et al., 2016), (Serra et al., 2003), and as a consequence of the partial devitrification that occurs in the last step of the synthesis. These peaks are located at 2θ of 24.9°, 44.6°, 48.9° and 49.7°.

On the other hand, it has been observed by some authors the formation of a new small peak at 2θ of 31.7° corresponding to high sintering temperatures that suggests the formation of a new secondary crystalline phase which was identified as silicorerhenanite $Na_2Ca_4(PO_4)_2SiO_4$ (Macías Andrés, 2016). In the 45S5 bioglass, phosphorus tends to depolymerise the silicon lattice and enter as a quadruple cation in the lattice (Lefebvre et al., 2007).

Graph 2 shows the FT-IR spectra of the 45S5 bioglass powders where two crystalline phases are observed, a sodium calcium silicate phase and a secondary phosphate phase (Bretcanu et al., 2009).

The FT-IR results of the 45S5 bioglass after the sintering process are shown below:

- Between 400 and 600 cm^{-1} we can observe the bending vibration bands of the Si–O–Si bonds.
- The bending mode signal of the P–O band is observed at 635 cm^{-1} (Peitl et al., 2001), (Vallet-Regí et al., 1999).
- The bands located approximately around 900 and 1100 cm-1 can be attributed to the Si–O and Si–O–Si stretching vibrations respectively (Peitl et al., 2001), (Filgueiras et al., 1993).

In summary, the levels of silicon present in the sample are optimal, as can be seen from the XRD and FT-IR tests, favouring the bonding and formation of the new bone, since the speed of the process can vary depending on the percentage of the element (being slower the higher the percentage of silicon in the glass, and may not even present direct bonding between the material and the bone) (Chen et al., 2008).

On the other hand, it has been observed that the high CaO/P_2O_5 ratio stimulates the reactivity of the bioglass surface in a physiological environment (Chen et al., 2008).

3.2. Characterisation of the samples

3.2.1. Viscosity and setting time

One of the fundamental parameters to be analysed in the formulation of this type of paste for scaffold injection moulding is the viscosity. Viscosity is a physical parameter of fluids that quantifies their resistance to movement. At the molecular level, viscosity is a measure of the friction existing between the particles that make up the fluid, given that the higher the viscosity, the more energy it will be necessary to invest in order to impart a certain speed to the flow.

Thus, when rheological tests were carried out, sample 1 (25%BGP/75% HA) was discarded as it presented a compact solid state with no capacity to flow.

By means of rheological measurements, the variation of viscosity with respect to shear rate was determined for the two remaining samples, as shown in Graph 3. The viscosity decreased with increasing shear rate, indicating a typically pseudoplastic profile, which coincides with

Table 1
Parameters of two different compositions studied.

	Parameter test for different samples	
	Sample 2	Sample 3
k	5.61	5.15
n	0.22	0.20
R^2	0,9372	0,9934

Table 2
Setting times of two different compositions studied.

	Setting time test for different samples	
	Sample 2	Sample 3
CT (min)	29	42
ST (min)	36	50

that described in the literature (Steffe, 1996), (Elleuch et al., 2007). Increasing the shear rate causes irreversible damage to the structure (Kiani et al., 2008), (Towler et al., 2007).

The consistency coefficient K and the flow behaviour index n of the specimens are given in Table 1.

The parameter n indicates the degree of deviation from the Newtonian behaviour of the fluids, when it is less than unity, 1, the fluid is non-Newtonian, and when this value is less than 0.7 it is pseudoplastic, therefore samples 2 and 3 fulfil both requirements.

The flow consistency factor K can be described identically to the concept of plastic viscosity since an increase in K indicates an increase in solids concentration. It indicates the consistency of the fluid, i.e., if the value of K is high, the fluid is more "viscous" and vice versa. In view of the results in Table 1, sample 3 has the lowest viscosity and could be optimal for filling the scaffold.

In summary, the flow properties are significantly affected by the percentage of HA, which leads to a decrease in the consistency coefficient K and the flow behaviour index n as the proportion of HA decreases (Eseller-Bayat et al., 2013).

The study of the cohesion time (CT) and setting time (ST) of the prepared samples (Table 2) is of great importance to determine the handling time of the samples and their ability to flow with a given consistency by an injector.

In view of the results, it is observed that the CT is lower than the ST, which allows the sample manipulation until the time of 3D printing (D'urso et al., 2000). Previous studies by M. D. Vlad in 2012 (Vlad et al., 2012), established that the Ca/P ratio exerted a significant influence on ST setting times, so the lower the HA ratio, the more homogeneous cohesion and uniform setting were observed.

From these results it can be seen that sample 3 has better starting properties and was selected for the rest of the test.

3.3. Characterisation of the scaffold (Hollow PLA Cube)

3.3.1. Porosity

The existence of pores in the scaffold is necessary to allow the migration and proliferation of osteoblasts and mesenchymal cells, and to promote vascularisation (Zeimaran et al., 2015), (Gerhardt and Boccaccini, 2010).

Generally, pores with an average diameter of 100 μm and porosity <50% (Fu et al., 2011b), (Rahaman et al., 2011) are considered to be the minimum requirements for tissue growth and functionality of scaffolds.

The fabrication of porous scaffolds as a support medium for tissue growth is key to facilitating the diffusion of nutrients and oxygen, as well as the removal of metabolic waste (Loh and Choong, 2013). The control of pore size is one of the parameters that most affect the mechanical properties of the structure, as well as its cell affinity. Thus, in addition to the pore size, it is interesting to determine the overall porosity values of the structure. For this purpose, a method based on the determination of the bulk density of printed parts and its comparison with the density of the solid material has been used. This procedure is widely used in the study of the porosity of parts obtained by additive manufacturing (equation (2.4)) (Domingos et al., 2013), (Domingos et al., 2012).

Taking into account that the density of PLA is 1.25 g cm^{-3}, and the density of the porous scaffold is 0.25 g cm^{-3}, this resulted in a porosity of 80%, which is considered optimal for this type of process.

Table 3
Average values of mechanical properties studied on the PLA 3D printed filled with injectable paste composites.

	Mechanical test	
	Young's Modulus [MPa]	Compressive strength [MPa]
PLA Filling	20000	510
Hollow PLA 80%	433,6	11,44

3.3.2. Mechanical properties of the scaffold

The biocompatibility of PLA has been proven since the 1970s and its use is widely reported in the literature (Schneider et al., 2010), (Hench et al., 1971), (Poh et al., 2013), (Qi et al., 2014). According to its biocompatibility and use, the PLA scaffold was fabricated as described above, and its mechanical properties were assessed.

The mechanical properties that PLA scaffolds possess decide their application. In our work, it is intended that the mechanical properties of the PLA scaffold should be as close as possible to the properties of the host bone for adequate load transfer to adjacent tissues (Costa-Pinto et al., 2011), (Saravanan et al., 2016).

Considering the mechanical properties observed in Graph 4 and Table 3 of the cube-shaped scaffold made of PLA with 20% filler, they show a modulus of elasticity of 433.60 MPa and a compressive strength of Rc = 11.44 MPa, so we can state that PLA scaffold has a disadvantage when used in tissue engineering due to a lower mechanical strength than normal bone (Lee et al., 2014), (Rodríguez-Vázquez et al., 2015).

Therefore, scaffold has poor mechanical properties and it is necessary to combine it with another natural or synthetic polymer or other type of material to provide better mechanical properties (Beladi et al., 2017).

3.4. Characterisation of the filled scaffold

In accordance with the previous section, and in order to improve the results obtained, the PLA Scaffold was filled with a paste composed of HA and BG 45S5.

HA has been widely studied for its biocompatibility and osteogenic potential, which has led it to be used as a material for grafts in bone defects. BG 45S5 has been the most extensively investigated glass in biomedical applications. BG also possesses the great property of chemically bonding to bone tissue. Its bonding to bone is attributed to the formation of a biologically active carbonate hydroxyapatite (CAH) layer on the surface of the BG when in contact with body fluid, which generates the bond between the living tissue and the biomaterial. Combining these three materials in the form of a filled scaffold blends the properties of the materials, enhancing their potential use in tissue engineering (Altamirano et al., 2016; Hench and Polak, 2002; Hench, 1998).

3.4.1. Properties of the filled scaffold

To improve the mechanical characteristics of the scaffold, it was filled with a mixture of bioglass and hydroxyapatite, and its mechanical properties were evaluated (Fig. 5).

Young's modulus, also known as the modulus of longitudinal elasticity, is a constant that materials possess that reflects the degree of elasticity that a given material possesses. Materials with higher Young's modulus are less elastic, i.e. stiffer, and materials with lower Young's modulus have higher elasticity. Therefore, in view of the results obtained for the PLA and filled PLA scaffold, it follows that the latter is more elastic than the PLA scaffold.

The scaffold must provide the cells with a three-dimensional structure and appropriate mechanical support for adhesion and proliferation, allowing growth into a suitable biomimetic functional structure (Little et al., 2011). In particular, biomaterials applied to bone tissue repair must have mechanical properties similar to bone tissue. Therefore, our results suggest that sample 3 exhibited an elastic modulus that is

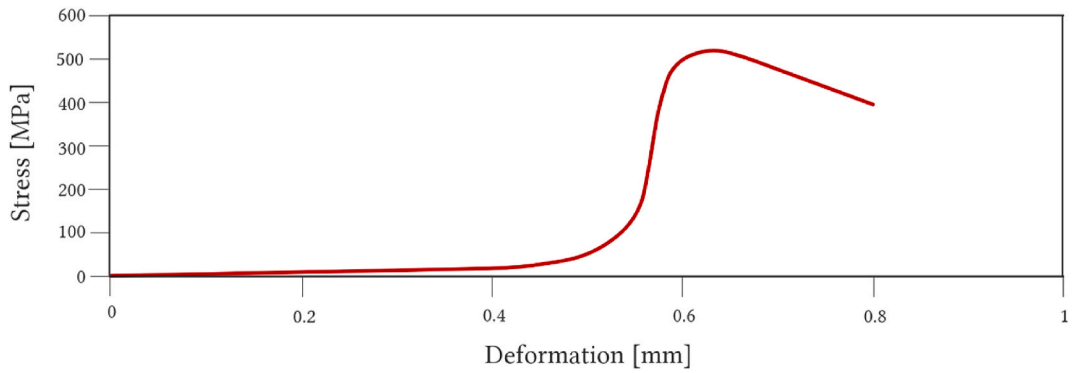

Graph 5. Stress-strain of hollow PLA + sample 3.

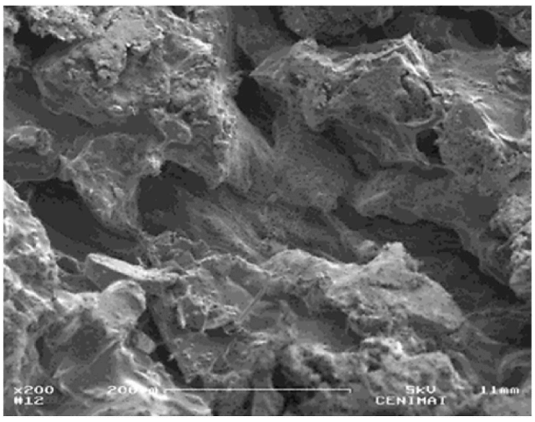

Fig. 3. SEM image of reference scaffold with 200x ampliation.

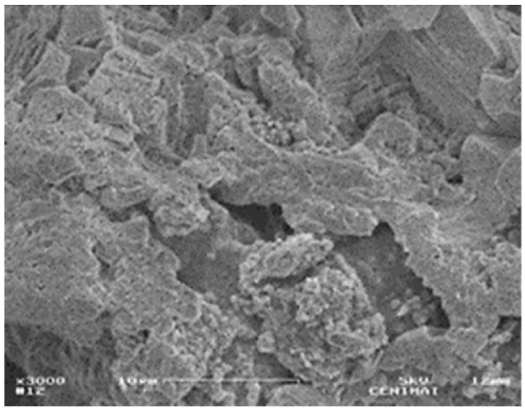

Fig. 4. SEM image of 1-day SBF scaffold with 3000x ampliation.

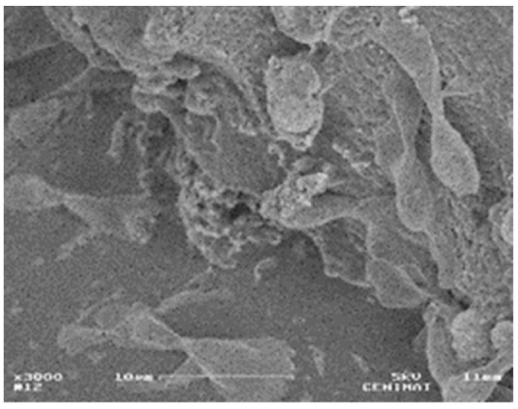

Fig. 5. SEM image of 3-day SBF scaffold with 3000x ampliation.

appropriate for use in this area. Considering that bone tissue is organised into cancellous bone (about 20% of the total skeleton) and cortical or compact bone (about 80% of the total skeleton), the proportions of these two architectural forms differ at various locations in the skeleton. Cortical bone is almost solid, with 10% porosity, while trabecular bone has porosity between 50 and 90%, making its modulus and maximum compressive strength approximately 20 times lower than that of cortical bone (Salgado et al., 2004). In vitro, scaffolds must have sufficient mechanical strength to withstand hydrostatic pressures and to maintain the spaces necessary for cell growth and matrix production (Leong et al., 2003).

In addition, the rate of scaffold degradation must be appropriately matched to the rate of new tissue growth, so that by the time the injury site is fully regenerated, the scaffold is fully degraded (Salgado et al., 2004).

Considering the mechanical properties observed in Graph 5 and Table 3, when comparing the Young's modulus of cortical bone (15 GPa) (Al-Barqawi et al., 2022) with that of the samples analysed, it can be observed that the value offered by sample 3 (20 GPa) is higher, which means that the scaffold has as much mechanical strength as the bone. Therefore, these scaffolds can be used in bones exposed to stress.

As can be seen in Table 3, the combination of the written materials to generate a filled scaffold presents very interesting properties compared to those found in the literature (Cannillo et al., 2010; Li et al., 2014; Seidenstuecker et al., 2017; Haghighi et al., 2021).

When comparing the Young's modulus of cortical bone (15 GPa) (Al-Barqawi et al., 2022), with that of the samples analysed, it is observed that the value offered by sample 3 (20 GPa) is higher, which means that the scaffold has as much mechanical strength as the bone. Therefore, these scaffolds can be used in bones exposed to stresses.

3.4.2. Assessment of the bioactivity of the filled scaffold

The bioactivity of the filled scaffolds was evaluated by immersion in simulated body fluid (SBF) and subsequent SEM analysis. For this, five trials were prepared with sample 3 and introduced into the PLA scaffolds. The first sample was not immersed in SBF, and was used as a reference sample. The rest of the samples were immersed in SBF for 1, 3, 5 and 7 days respectively (Figs. 3–7).

The SEM images corresponding to Fig. 3 (reference sample without contact with SBF) show an irregular surface with the presence of pores of different sizes. Also, the presence of hydroxyapatite can be observed, probably on the bioglass. In the following images we can already see the growth of hydroxyapatite on the surface, a process that takes place over the course of the days of contact of the SBF with the samples, until the

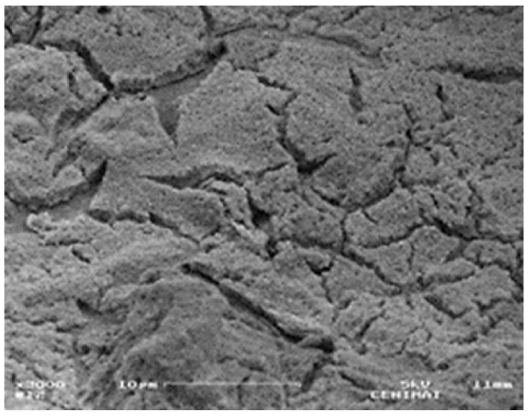

Fig. 6. SEM image of 5-day SBF scaffold with 3000x ampliation.

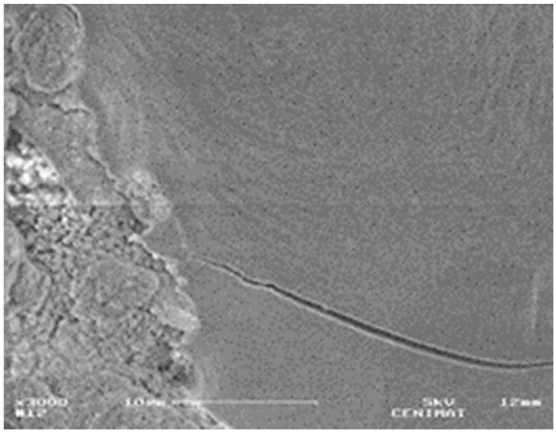

Fig. 7. SEM image of 7-day SBF scaffold with 3000x ampliation.

formation of the thick layer of calcium phosphate that can be seen in Fig. 7. This shows the optimal behaviour of the substrate under biological conditions.

4. Discussion

The use of Bioglass® 45S5 in tissue engineering has been widely studied due to its versatility and good properties. Bioglass forms a silica gel very quickly in a biological environment, which allows calcium phosphates to strongly adhere and grow on its surface. Hydroxyapatite is another commonly used material in tissue engineering, as it is the main component of bones and teeth. Scaffolds filled with natural inorganic components like hydroxyapatite have circumstantial biological or physiological functions. Calcium phosphate, which is the main component of hydroxyapatite, has positive effects on osteoblast proliferation and adhesion due to its chemical structure comparable to that of human bone.

In this study, an injectable paste was produced by combining Bioglass® 45S5 and hydroxyapatite on a 3D printed porous structure using a thermoplastic (PLA). The mechanical and bioactive properties of the scaffold were evaluated, and the results showed that the scaffold had good mechanical strength, which is essential for bone regeneration applications. Additionally, the scaffold exhibited excellent bioactivity due to the presence of both bioglass and hydroxyapatite.

The results of this study demonstrate the potential of an injectable paste of Bioglass® 45S5 and hydroxyapatite on a 3D printed porous structure for use in regenerative medicine.

5. Conclusion

After characterising the two samples, the following conclusions were reached:

- Samples 2 and 3 presented a decrease in viscosity with increasing shear rate, this being a typical behaviour of a non-Newtonian material, but sample 3 presented a higher linearity and a lower dispersion of the data provided. In addition, this sample has a longer setting time compared to sample 2. In view of these results, sample 3 is more suitable for the requirements of this work as it has an easier injection from the start, so it is the one used in the rest of the work.
- The porosity of 80% obtained as a result of filling the PLA cube with the BGP + HA paste was appropriate for carrying out the experiment, as this value is considered optimal for this type of process.
- Sample 3 has a Young's modulus of 20 GPa (Table 3), higher than that of cortical bone, so that the scaffolds generated with this paste, in origin, have sufficient mechanical strength to be used in possible bone implants.

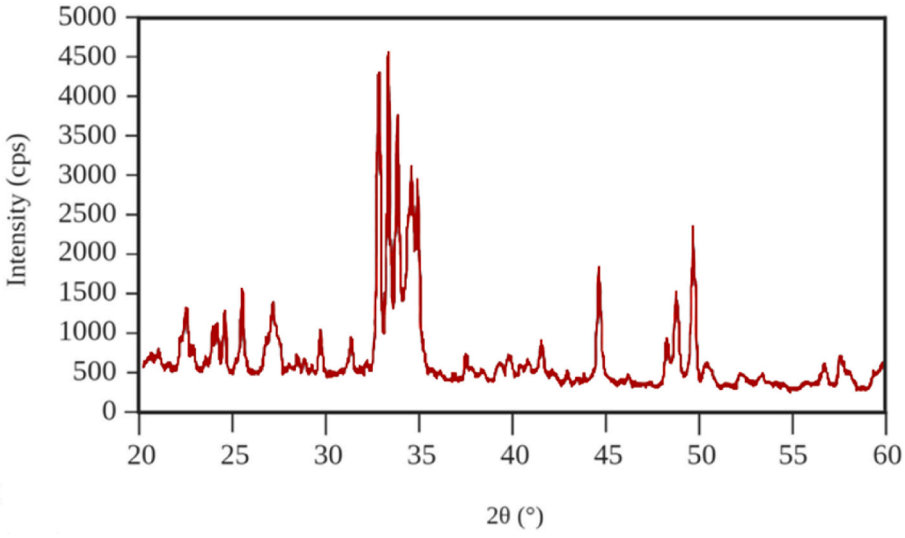

Graph 1. X-ray Diffraction (XRD) results of the Bioglass powders.

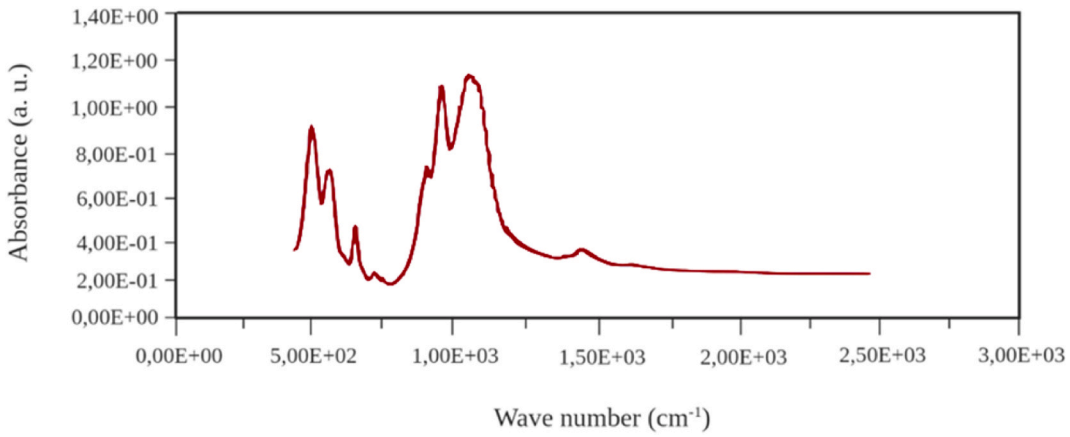

Graph 2. FTIR diffractogram of the Bioglass powders.

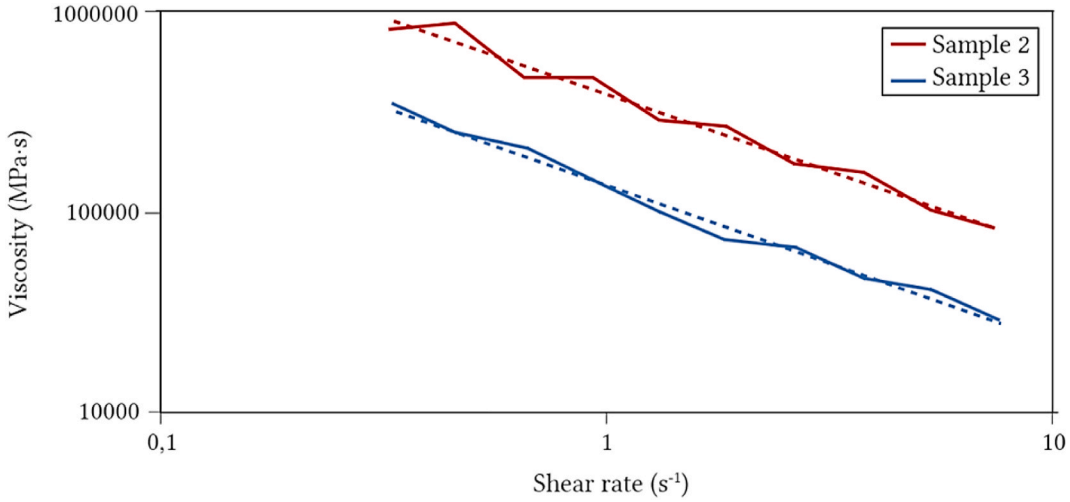

Graph 3. Viscosity of two different compositions studied.

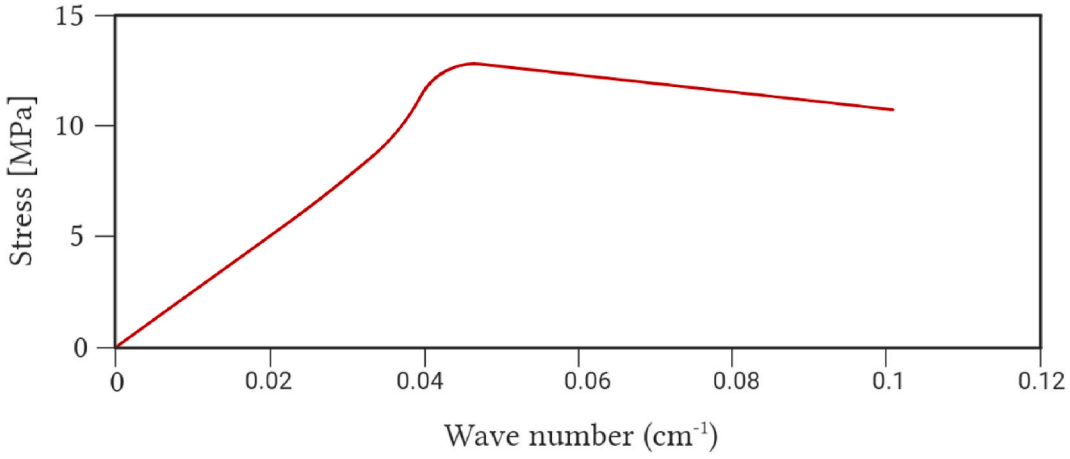

Graph 4. Stress-strain of hollow PLA.

- The bioactivity results were really promising, as the samples immersed in SBF for 1, 5 and 7 days respectively showed cell growth on the surface, and even in the sample immersed for 7 days a stacked cell growth was observed. This event demonstrates the optimal behaviour of the substrate under biological conditions.
- Following the above results, it can be concluded that this work demonstrates that, although some studies with similar pastes had already been carried out, they had never been carried out with this application and in combination with PLA structures. This particular mixture of materials can be developed for high precision scaffolds.

The results showed very interesting mechanical and bioactivity properties for use in bone implants.

Compliance with ethics guidelines

Jesús M. Rodríguez-Rego, Laura Mendoza-Cerezo, Anabel Soriano-Carrera, Alfonso C. Marcos-Romero, Antonio Macías-García declare that they have no conflict of interest.

This article does not contain any studies with human or animal subjects performed by any of the authors.

CRediT authorship contribution statement

Laura Mendoza-Cerezo: Writing – original draft. **Jesús M. Rodríguez-Rego:** Writing – original draft, Methodology, Investigation. **Anabel Soriano-Carrera:** Investigation. **Alfonso C. Marcos-Romero:** Validation, Funding acquisition. **Antonio Macías-García:** Writing – review & editing, Visualization, Validation, Supervision, Methodology.

Declaration of competing interest

The authors declare that they have no known competing financial interests or personal relationships that could have appeared to influence the work reported in this paper.

Data availability

Data will be made available on request.

Acknowledgements

This research has been funded by the European Regional Development Fund (FEDER) in the framework of the project (BIOSIMPRO. IB20158) with the code 2021/00110/001 for funding this publication.

References

Aguilar-Reyes, E.A., León-Patiño, C.A., Jacinto-Diaz, B., Lefebvre, L.P., 2012. Structural characterization and mechanical evaluation of bioactive glass 45S5 foams obtained by a powder technology approach. J. Am. Ceram. Soc. 95 (12), 3776–3780. https://doi.org/10.1111/J.1551-2916.2012.05465.X.

Al-Barqawi, M.O., Church, B., Thevamaran, M., Thoma, D.J., Rahman, A., 2022. Design and validation of additively manufactured metallic cellular scaffold structures for bone tissue engineering. Materials 15 (9), 3310. https://doi.org/10.3390/MA15093310, 2022, Vol. 15, Page 3310.

Altamirano, A.A., et al., 2016. Biocompatibility of nanofibrous scaffolds with different concentrations of PLA/hydroxyapatite. Odovtos - International Journal of Dental Sciences 18 (3), 39–50. https://doi.org/10.15517/IJDS.V0I0.25987.

Bai, X., Gao, M., Syed, S., Zhuang, J., Xu, X., Zhang, X.Q., 2018. Bioactive hydrogels for bone regeneration. Bioact. Mater. 3 (4), 401–417. https://doi.org/10.1016/J.BIOACTMAT.2018.05.006.

Baino, F., Vitale-Brovarone, C., 2011. Three-dimensional glass-derived scaffolds for bone tissue engineering: current trends and forecasts for the future. J. Biomed. Mater. Res. 97 (4), 514–535. https://doi.org/10.1002/JBM.A.33072.

Beladi, F., Saber-Samandari, S., Saber-Samandari, S., 2017. Cellular compatibility of nanocomposite scaffolds based on hydroxyapatite entrapped in cellulose network for bone repair. Mater Sci Eng C Mater Biol Appl 75, 385–392. https://doi.org/10.1016/J.MSEC.2017.02.040.

Bretcanu, O., Chatzistavrou, X., Paraskevopoulos, K., Conradt, R., Thompson, I., Boccaccini, A.R., 2009. Sintering and crystallisation of 45S5 Bioglass® powder. J. Eur. Ceram. Soc. 29 (16), 3299–3306. https://doi.org/10.1016/J.JEURCERAMSOC.2009.06.035.

Cannillo, V., Chiellini, F., Fabbri, P., Sola, A., 2010. Production of Bioglass® 45S5 – polycaprolactone composite scaffolds via salt-leaching. Compos. Struct. 92 (8), 1823–1832. https://doi.org/10.1016/J.COMPSTRUCT.2010.01.017.

Chen, Q., Roether, J., Boccaccini, A., 2008. Tissue engineering scaffolds from bioactive glass and composite materials. Mater. Sci.

Costa-Pinto, A.R., Reis, R.L., Neves, N.M., 2011. Scaffolds based bone tissue engineering: the role of chitosan. Tissue Eng. B Rev. 17 (5), 331–347. https://doi.org/10.1089/TEN.TEB.2010.0704.

Cuende, N., 2013. Andalusian initiative for advanced therapies: fostering synergies. Stem. Cells Transl. Med. 2 (4), 243–245. https://doi.org/10.5966/sctm.2013-0051.

Domingos, M., Chiellini, F., Gloria, A., Ambrosio, L., Bartolo, P., Chiellini, E., 2012. Effect of process parameters on the morphological and mechanical properties of 3D Bioextruded poly(1-caprolactone) scaffolds. Rapid Prototyp. J. 18 (1), 56–67. https://doi.org/10.1108/13552541211193502/FULL/XML.

Domingos, M., et al., 2013. Improved osteoblast cell affinity on plasma-modified 3-D extruded PCL scaffolds. Acta Biomater. 9 (4), 5997–6005. https://doi.org/10.1016/J.ACTBIO.2012.12.031.

Donnelly, E., Boskey, A.L., 2011. Mineralization. In: Feldman, D., Pike, J.W., Adams, J.S. (Eds.), Vitamin D: Two-Volume Set. Academic Press, pp. 381–401. https://doi.org/10.1016/B978-0-12-381978-9.10021-6.

D'urso, P.S., et al., 2000. Custom cranioplasty using stereolithography and acrylic. Br. J. Plast. Surg. 53 (3), 200–204. https://doi.org/10.1054/bjps.1999.3268.

Elleuch, M., Besbes, S., Roiseux, O., Blecker, C., Attia, H., 2007. Quality characteristics of sesame seeds and by-products. Food Chem. 103 (2), 641–650. https://doi.org/10.1016/J.FOODCHEM.2006.09.008.

Eseller-Bayat, E., Gokyer, S., Yegian, M.K., Deniz, R.O., Alshawabkeh, A., 2013. Bender elements and bending disks for measurement of shear and compression wave velocities in large fully and partially saturated sand specimens. Geotech. Test J. 36 (2) https://doi.org/10.1520/GTJ20120024.

Faber, J., Berto, P.M., Quaresma, M., 2006. Rapid prototyping as a tool for diagnosis and treatment planning for maxillary canine impaction. Am. J. Orthod. Dentofacial Orthop. 129 (4), 583–589. https://doi.org/10.1016/j.ajodo.2005.12.015.

I. Farooq, Z. Imran, U. Farooq, A. Leghari, and H. Ali, "Bioactive glass: a material for the future," World J. Dent., vol. 3, no. 2, pp. 199–201, doi: 10.5005/jp-journals-10015-1156.

Fávaro-Pípi, E., et al., 2011. Low-level laser therapy induces differential expression of osteogenic genes during bone repair in rats. Photomed. Laser Surg. 29 (5), 311–317. https://doi.org/10.1089/pho.2010.2841.

Filgueiras, M.R.T., la Torre, G., Hench, L.L., 1993. Solution effects on the surface reactions of three bioactive glass compositions. J. Biomed. Mater. Res. 27 (12), 1485–1493. https://doi.org/10.1002/JBM.820271204.

Filová, E., et al., 2014. Support for the initial attachment, growth and differentiation of MG-63 cells: a comparison between nano-size hydroxyapatite and micro-size hydroxyapatite in composites. Int. J. Nanomed. 9 (1), 3687–3706. https://doi.org/10.2147/IJN.S56661.

Fu, Q., Saiz, E., Rahaman, M.N., Tomsia, A.P., 2011a. Bioactive glass scaffolds for bone tissue engineering: state of the art and future perspectives. Mater Sci Eng C Mater Biol Appl 31 (7), 1245. https://doi.org/10.1016/J.MSEC.2011.04.022.

Fu, Q., Saiz, E., Rahaman, M.N., Tomsia, A.P., 2011b. Bioactive glass scaffolds for bone tissue engineering: state of the art and future perspectives. Mater Sci Eng C Mater Biol Appl 31 (7), 1245–1256. https://doi.org/10.1016/J.MSEC.2011.04.022.

Gerhardt, L.C., Boccaccini, A.R., 2010. Bioactive glass and glass-ceramic scaffolds for bone tissue engineering. Materials 3 (7), 3867. https://doi.org/10.3390/MA3073867.

Haghighi, F.D., Beidokhti, S.M., Najaran, Z.T., Sahebian Saghi, S., 2021. Highly improved biological and mechanical features of bioglass-ceramic/gelatin composite scaffolds using a novel silica coverage. Ceram. Int. 47 (10), 14048–14061. https://doi.org/10.1016/J.CERAMINT.2021.01.274.

Hench, L.L., 1998. Bioceramics. In: Journal of the American Ceramic Society. John Wiley & Sons, Ltd, pp. 1705–1728. https://doi.org/10.1111/J.1151-2916.1998.TB02540.X.

Hench, L.L., 2013. Chronology of bioactive glass development and clinical applications. New J. Glass Ceram. 3 (2), 67–73. https://doi.org/10.4236/NJGC.2013.32011.

Hench, L.L., Polak, J.M., 2002. Third-generation biomedical materials. Science 295 (5557). https://doi.org/10.1126/SCIENCE.1067404.

Hench, L.L., Splinter, R.J., Allen, W.C., Greenlee, T.K., 1971. Bonding mechanisms at the interface of ceramic prosthetic materials. J. Biomed. Mater. Res. 5 (6), 117–141. https://doi.org/10.1002/JBM.820050611.

Jonasova, L., Helebrant, A., Ludvik, S., 2002. The Influence of Simulated Body Fluid Composition on Carbonated Hydroxyapatite Formation. Ceramics Silikaty [Online]. Available: https://www.researchgate.net/publication/282061103_The_influence_of_simulated_body_fluid_composition_on_carbonated_hydroxyapatite_formation. (Accessed 22 November 2022).

Jones, J.R., 2015. Reprint of: review of bioactive glass: from Hench to hybrids. Acta Biomater. 23 (S), S53–S82. https://doi.org/10.1016/J.ACTBIO.2015.07.019. Suppl.

Kiani, H., Mousavi, S.M.A., Emam-Djomeh, Z., 2008. Rheological properties of Iranian yoghurt drink, Doogh. Int. J. Dairy Sci. 3 (2), 71–78. https://doi.org/10.3923/IJDS.2008.71.78.

Kokubo, T., 1991. Bioactive glass ceramics: properties and applications. Biomaterials 12 (2), 155–163. https://doi.org/10.1016/0142-9612(91)90194-F.

Kokubo, T., Takadama, H., 2006. How useful is SBF in predicting in vivo bone bioactivity? Biomaterials 27 (15), 2907–2915. https://doi.org/10.1016/J.BIOMATERIALS.2006.01.017.

Langer, R., Vacanti, J.P., 1993. Tissue engineering. Science 260 (5110), 920–926. https://doi.org/10.1126/SCIENCE.8493529.

Lee, J.S., et al., 2014. In vivo study of chitosan-natural nano hydroxyapatite scaffolds for bone tissue regeneration. Int. J. Biol. Macromol. 67, 360–366. https://doi.org/10.1016/J.IJBIOMAC.2014.03.053.

Lefebvre, L., et al., 2007. Structural transformations of bioactive glass 45S5 with thermal treatments. Acta Mater. 55 (10), 3305–3313. https://doi.org/10.1016/J.ACTAMAT.2007.01.029.

Leong, K.F., Cheah, C.M., Chua, C.K., 2003. Solid freeform fabrication of three-dimensional scaffolds for engineering replacement tissues and organs. Biomaterials 24 (13), 2363–2378. https://doi.org/10.1016/S0142-9612(03)00030-9.

Li, R., Clark, A.E., Hench, L.L., 1991. An investigation of bioactive glass powders by sol-gel processing. J. Appl. Biomater. 2 (4), 231–239. https://doi.org/10.1002/JAB.770020403.

Li, W., Nooeaid, P., Roether, J.A., Schubert, D.W., Boccaccini, A.R., 2014. Preparation and characterization of vancomycin releasing PHBV coated 45S5 Bioglass®-based glass–ceramic scaffolds for bone tissue engineering. J. Eur. Ceram. Soc. 34 (2), 505–514. https://doi.org/10.1016/J.JEURCERAMSOC.2013.08.032.

Little, C.J., Bawolin, N.K., Chen, X., 2011. Mechanical properties of natural cartilage and tissue-engineered constructs. Tissue Eng. B Rev. 17 (4), 213–227. https://doi.org/10.1089/TEN.TEB.2010.0572.

Loh, Q.L., Choong, C., 2013. Three-dimensional scaffolds for tissue engineering applications: role of porosity and pore size. Tissue Eng. B Rev. 19 (6), 485–502. https://doi.org/10.1089/TEN.TEB.2012.0437.

Macías Andrés, V.I., 2016. Estudio de bioactividad in vitro de espumas de biovidrio 45S5 producidas por tecnología de polvos para aplicaciones en regeneración ósea. Universidad Michoacana de San Nicolás de Hidalgo, Michoacán [Online]. Available: http://bibliotecavirtual.dgb.umich.mx:8083/xmlui/bitstream/handle/DGB_UMICH/1309/IIMM-D-2016-1330.pdf?sequence=1&isAllowed=y. (Accessed 4 February 2023).

Mavili, M.E., Canter, H.I., Saglam-Aydinatay, B., Kamaci, S., Kocadereli, I., 2007. Use of three-dimensional medical modeling methods for precise planning of orthognathic surgery. J. Craniofac. Surg. 18 (4), 740–747. https://doi.org/10.1097/scs.0b013e318069014f.

Nandiyanto, A.B.D., Oktiani, R., Ragadhita, R., 2019. How to read and interpret ftir spectroscope of organic material. Indonesian J. Sci. Technol. 4 (1), 97–118. https://doi.org/10.17509/IJOST.V4I1.15806.

Peitl, O., Dutra Zanotto, E., Hench, L.L., 2001. Highly bioactive P2O5-Na2O-CaO-SiO2glass-ceramics. J. Non-Cryst. Solids 292 (1–3), 115–126. https://doi.org/10.1016/S0022-3093(01)00822-5.

Poh, P.S.P., Hutmacher, D.W., Stevens, M.M., Woodruff, M.A., 2013. Fabrication and in vitro characterization of bioactive glass composite scaffolds for bone regeneration. Biofabrication 5 (4), 045005. https://doi.org/10.1088/1758-5082/5/4/045005.

Qi, C., Zhu, Y.J., Ding, G.J., Wu, J., Chen, F., 2014. Solvothermal synthesis of hydroxyapatite nanostructures with various morphologies using adenosine 5′-monophosphate sodium salt as an organic phosphorus source. RSC Adv. 5 (5), 3792–3798. https://doi.org/10.1039/C4RA13151G.

Rahaman, M.N., et al., 2011. Bioactive glass in tissue engineering. Acta Biomater. 7 (6), 2355–2373. https://doi.org/10.1016/J.ACTBIO.2011.03.016.

Rámila, A., Vallet-Regí, M., 2001. Static and dynamic in vitro study of a sol-gel glass bioactivity. Biomaterials 22 (16), 2301–2306. https://doi.org/10.1016/S0142-9612(00)00419-1.

Rodríguez-Vázquez, M., Vega-Ruiz, B., Ramos-Zúñiga, R., Saldaña-Koppel, D.A., Quiñones-Olvera, L.F., 2015. Chitosan and its potential use as a scaffold for tissue engineering in regenerative medicine. BioMed Res. Int. 2015 https://doi.org/10.1155/2015/821279.

Salahuddin, N., Ibrahim, E.M., El-Kemary, M., 2022. Different methods for preparation of hydroxyapatite nanostructures. Biointerface Res. Appl. Chem. 13 (3), 236. https://doi.org/10.33263/BRIAC133.236.

Salgado, A.J., Coutinho, O.P., Reis, R.L., 2004. Bone tissue engineering: state of the art and future trends. Macromol. Biosci. 4 (8), 743–765. https://doi.org/10.1002/MABI.200400026.

Sanders, D.M., Person, W.B., Hench, L.L., 2016, 10.1366/000370274774332623. Quantitative Analysis of Glass Structure with the Use of Infrared Reflection Spectra, vol. 21, pp. 247–255. https://doi.org/10.1366/000370274774332623, 3.

Saravanan, S., Leena, R.S., Selvamurugan, N., 2016. Chitosan based biocomposite scaffolds for bone tissue engineering. Int. J. Biol. Macromol. 93 (Pt B), 1354–1365. https://doi.org/10.1016/J.IJBIOMAC.2016.01.112.

Schneider, C.K., et al., 2010. Challenges with advanced therapy medicinal products and how to meet them. Nat. Rev. Drug Discov. 9 (3), 195–201. https://doi.org/10.1038/nrd3052. Nature Publishing Group.

Seidenstuecker, M., et al., 2017. 3D powder printed bioglass and β-tricalcium phosphate bone scaffolds. Materials 11 (1), 13. https://doi.org/10.3390/MA11010013, 2018, Vol. 11, Page 13.

Serra, J., et al., 2003. FTIR and XPS studies of bioactive silica based glasses. JNCS 332 (1), 20–27. https://doi.org/10.1016/J.JNONCRYSOL.2003.09.013.

Serra, T., Mateos-Timoneda, M.A., Planell, J.A., Navarro, M., 2013. 3D printed PLA-based scaffolds: a versatile tool in regenerative medicine • 3D printed PLA-based scaffolds • A versatile tool in regenerative medicine. Organogenesis 9 (4), 239. https://doi.org/10.4161/ORG.26048.

Shor, L., et al., 2009. Precision extruding deposition (PED) fabrication of polycaprolactone (PCL) scaffolds for bone tissue engineering. Biofabrication 1 (1). https://doi.org/10.1088/1758-5082/1/1/015003.

Sima, F., Ristoscu, C., Duta, L., Gallet, O., Anselme, K., Mihailescu, I.N., 2016. Laser thin films deposition and characterization for biomedical applications. In: Vilar, R. (Ed.), Laser Surface Modification of Biomaterials: Techniques and Applications. Woodhead Publishing, pp. 77–125. https://doi.org/10.1016/B978-0-08-100883-6.00003-4.

Steffe, J.F., 1996. Rheological methods in food process engineering. In: Agricultural Engineering, pp. 1–412 [Online]. Available: http://linkinghub.elsevier.com/retrieve/pii/0260877494900906. (Accessed 5 February 2023).

Towler, B.W., Cunningham, A., Stoodley, P., McKittrick, L., 2007. A model of fluid–biofilm interaction using a Burger material law. Biotechnol. Bioeng. 96 (2), 259–271. https://doi.org/10.1002/BIT.21098.

Vallet-Regí, M., Romero, A.M., Ragel, C., Legeros, R., 1999. XRD, SEM-EDS, and FTIR studies of in vitro growth of an apatite-like layer on sol-gel glasses. J. Biomed. Mater. Res. https://doi.org/10.1002/(SICI)1097-4636(19990315)44:4.

Vlad, M.D., Gómez, S., Barracó, M., López, J., Fernández, E., 2012. Effect of the calcium to phosphorus ratio on the setting properties of calcium phosphate bone cements. J. Mater. Sci. Mater. Med. 23 (9), 2081–2090. https://doi.org/10.1007/S10856-012-4686-3/METRICS.

Wang, A., Wang, W., 2009. Superabsorbent materials. Kirk-Othmer Encyclopedia of Chemical Technology. https://doi.org/10.1002/0471238961.SUPEWANG.A01.

Wang, F., Cai, X., Shen, Y., Meng, L., 2023. Cell–scaffold interactions in tissue engineering for oral and craniofacial reconstruction. Bioact. Mater. 23, 16–44. https://doi.org/10.1016/J.BIOACTMAT.2022.10.029.

Zeimaran, E., Pourshahrestani, S., Djordjevic, I., Pingguan-Murphy, B., Kadri, N.A., Towler, M.R., 2015. Bioactive glass reinforced elastomer composites for skeletal regeneration: a review. Mater. Sci. Eng. C 53, 175–188. https://doi.org/10.1016/J.MSEC.2015.04.035.

Injertos sustitutos no óseos: aportaciones del ácido poliláctico y poliglicólico. https://scielo.isciii.es/scielo.php?script=sci_arttext&pid=S1699-65852009000100006. (Accessed 8 December 2022).

Objetivos conceptuales y metodológicos de la investigación histológica. http://scielo.isciii.es/scielo.php?script=sci_arttext&pid=S1575-18132004000200007. (Accessed 3 April 2021).

The Williams dictionary of biomaterials - D. F. Williams - google libros. https://books.google.es/books?hl=es&lr=&id=Hv45B7P5N3gC&oi=fnd&pg=PR5&ots=hPoU_jo3Xn&sig=f6ahRdDh0louKDaLbCXo4mwlZAk&redir_esc=y#v=onepage&q&f=false. (Accessed 3 April 2021).